

# THE EFFECT OF INTERPARTICLE COHESIVE FORCES ON THE SIMULATION OF FLUID FLOW IN SPOUT-FLUID BEDS

A. L. G. Trindade<sup>1</sup>, M. L. Passos<sup>1\*</sup>, E. F. Costa Jr.<sup>2</sup> and E. C. Biscaia Jr.<sup>2</sup>

<sup>1</sup>Curso de Pós-Graduação em Engenharia Química DEQ/EE/UFMG  
Rua Espírito Santo 35, 6º andar, Belo Horizonte - MG, Brasil.  
CEP 30160-030; Fax (31) 32381789  
E-mail: merilau@microplanet.com.br

<sup>2</sup>Programa de Engenharia Química COPPE/UF RJ, Fax (21) 5907135  
Cx. P. 68502, CEP 21945-970, Rio de Janeiro - RJ, Brasil.

(Received: April 15, 2003 ; Accepted: July 17, 2003)

**Abstract** - As reflected in the literature, solid-fluid flow characteristics in spouted beds can vary widely when particles are coated by a suspension. This work is aimed at describing the effect of interparticle forces on airflow distribution in conical spouted beds of inert particles coated by *Eucalyptus* black liquor. The simulator developed earlier is modified to incorporate this effect. Two corrective functions with adjustable parameters are introduced into the simulator gas-flow model to generate the minimum spouting conditions in beds wetted by this liquor. These functions are assumed to be dependent on characteristic suspension groups and bed height. Using the particle swarm optimization (PSO) technique, expressions for these functions are obtained. Simulated results are presented and discussed to validate this technique. Implications of these results on drying *Eucalyptus* black liquor in conical spouted beds are analyzed.

**Keywords:** *Eucalyptus* black liquor, cohesive forces, minimum spouting conditions.

## INTRODUCTION

*Eucalyptus* black liquor, a by-product of the Kraft process, was selected as the suspension for use in this work because of its importance in the pulp and paper industries. This liquor, which is composed of two thirds of organic matter, comes from the wood digester and behaves as a pseudoplastic fluid with high apparent viscosity at solids concentrations higher than 50 %, as shown in Figure 1. To be used as fuel, this liquor must be concentrated in the multiple-effect evaporator system from 14 % to about 75 % dry solids before feeding it into the recovery boiler. During its combustion and burning, enough steam is generated to supply about 80% of the total energy required by the industrial plant. Sodium carbonate and sulfite are also

recovered in this step, and after clarification and calcination, these inorganic components regenerate the white liquor for reuse in the digester.

Recent studies have demonstrated that the thermal efficiency of the boiler can be improved and polluted gas emissions can be reduced by feeding the recovery boiler with a more concentrated liquor, i.e.  $C_{ss} > 80$  % (Green and Hough, 1992; Hyoty and Ojala, 1988). Computer simulations of the Kraft recovery boiler corroborate a 10% increase in its thermal efficiency when the solids concentration of *Eucalyptus* black liquor is raised from 75 % to about 99.9 % (Cardoso, 1998). Moreover, as boiler temperature rises, chemical reactions between sulfur gases and sodium in the ashes are improved for sodium sulfate precipitation. This explains the

---

\*To whom correspondence should be addressed

reduction in polluted gas emissions. In addition, operation of the Kraft recovery boiler is safer when a concentrated liquor is processed (Smook, 1992).

Although there are technical, economic and environment advantages to working with a more concentrated black liquor, the use of multiple-effect evaporators to concentrate this liquor up to 75 % is restrained by its high viscosity. Different techniques to reduce *Pine* liquor viscosity before concentrating it have been proposed in the literature. These techniques, such as addition of salts, thermal treatment or pressurized tank storage (see Cardoso, 1998), are specific for softwood liquors and generally cannot be applied to hardwood liquors such as that of *Eucalyptus*.

Trindade et al. (2002) developed an alternative technique for concentrating *Eucalyptus* black liquor in a conical spouted bed of inert polypropylene particles. Their results for a semipilot unit prove the technical feasibility of producing *Eucalyptus* black liquor powder fuel with a 4 to 12 % moisture content

(dry basis) without any thermal degradation of its high heating (gross calorific) value. As pointed out by these authors, this technique is the most adequate for processing the liquor because the inert particle circulation inside the bed induces high shear rates in the thin liquor layer that covers the particle surface. This results in a significant reduction in the apparent viscosity of the liquor, as shown in Figure 1, enhancing the possibility of processing and drying the liquor. Rigid control of bed temperature helps to maintain the apparent viscosity of the liquor lower during the entire drying operation. Control of bed temperature and stable particle circulation avoid agglomeration and guarantee stable operation for producing powder and transporting it by air to the cyclone attached to the column exit. However, to improve the thermal efficiency of this dryer as well as its scale-up, it is necessary to make some modifications in its operation and in air recycling. This requires process simulations to select the best route for improving this equipment.

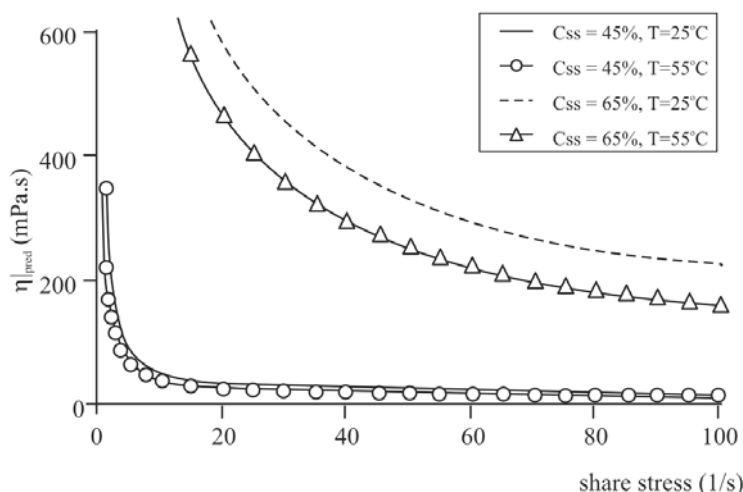


**Figure 1:** Apparent viscosity,  $\eta$ , of *Eucalyptus* black liquor as a function of the shear rates at different solids concentrations,  $C_{ss}$ , and temperatures,  $T$ . (Passos et al. 2000).

### Simulation of Drying Diluted Suspensions in Spout-Fluid Bed

Costa Jr. et al. (2001) developed a simulator for describing the drying of diluted suspensions in conical spout-fluid beds, neglecting the effect of interparticle forces on gas flow distribution. This simulator comprises three interactive modules that represent the numerical solution of the following models: gas flowing throughout the bed of inert particles (module 1); particle circulation inside the

spout, annulus and fountain regions (module 2) and drying of suspensions in these three regions (module 3). In this simulator, the input parameter data are as follows: the column dimensions ( $\alpha$ ,  $d_i$  and  $d_b$ ); the physical properties of inert particles ( $d_p$ ,  $\phi$ ,  $\rho_s$ ); the inlet airflow rate, temperature and humidity; the particle bed height ( $H$ ) and porosity ( $\epsilon_a = \epsilon_{mf}$ ); and the suspension flow rate and its specific drying properties. This computer program generates its own database for air properties as a function of air humidity and temperature. However, if another gas is

used as a drying medium, the program requests a new input database for the properties of this gas.

The program starts by running module 1. The gas-flow model is then solved and its output variables,  $Q_{mj}$ ,  $\Delta P_{mj}$ ,  $d_{mj}(z)$ ,  $\Delta P_j(z)$ ,  $U_a(z)$  and  $U_j(z)$ , are the input parameters of module 2. In this module, the solids circulation rate under the inlet airflow condition (that must be greater than  $Q_{mj}$ ) as well as the volumetric solids concentration along the bed height in the spout and fountain regions is obtained. These output variables together with those from module 1 enter into module 3, where mass and energy balance equations for the three phases (solid - gas - suspension) are solved together with the drying kinetic equation for the suspension. These two modules supply all data needed for describing the operation of drying diluted suspension.

Figure 2 displays a schematic representation of the gas-flow model. As seen, the bed of particles is divided into  $n$  cylindrical segments of the same height ( $H/n$ ). Each one of these segments is assumed to behave as a spout-fluid bed under aerated spouting flow regime. Air is injected into the bed through the nozzle attached to the central base of the column and through the lateral column area (up to  $H_L$  height). Spout diameter is supposed to be constant within each segment but it can vary from one segment to another. By solving the mass balance for the dry gas and the empirical equations for the spout-annulus interface location in each segment, data on annular superficial gas velocity and spout diameter are generated along the bed height. From these data, the minimum spouting conditions ( $Q_{mj}$  and  $\Delta P_{mj}$ ) are determined.

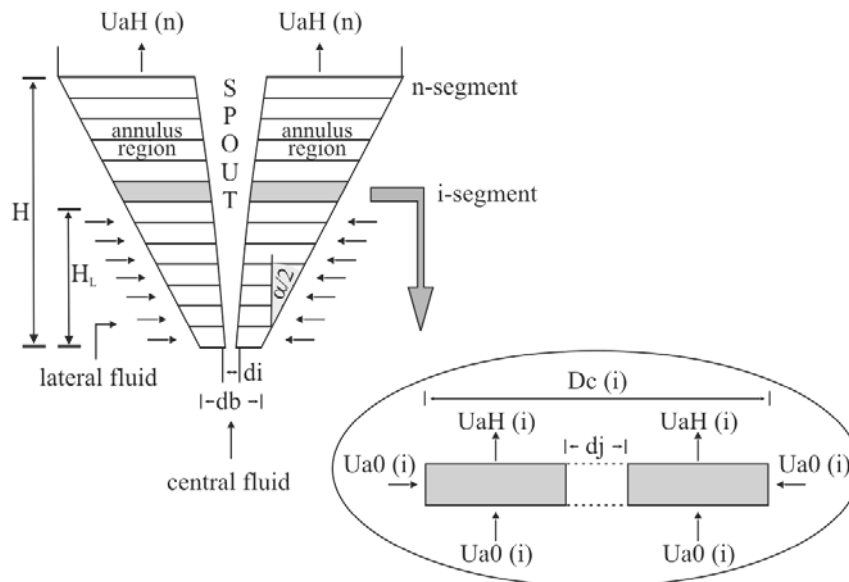


**Figure 2:** Schematic representation of gas flow model in conical spout-fluid beds. (Costa Jr. et al., 2001).

The main feature of this model is to predict gas flow behavior as a function of the spout formation mechanism, specified by the range of parameter  $A$ . This dimensionless parameter represents the ratio of the minimum inlet energy required to form the spout to the minimum frictional energy lost to sustain the spout throughout its area (Littman and Morgan, 1988):

$$A = \frac{\rho_f U_{mf} U_T}{(\rho_s - \rho_f) g d_i} \quad (1)$$

For each specified range of parameter  $A$  presented in Table 1,  $d_{mj}(z)$  and  $U_a(z)$  differ in shape.

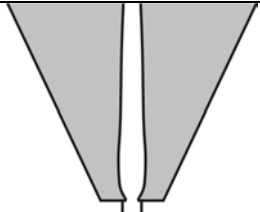
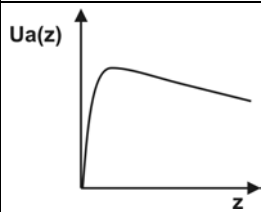
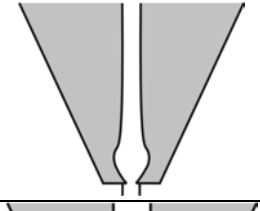
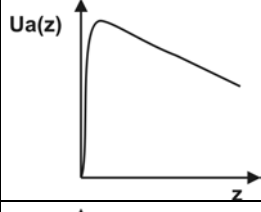
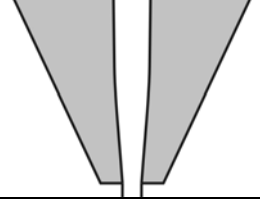
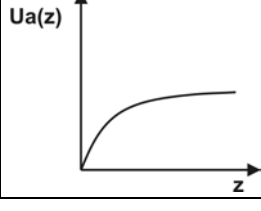
These results are corroborated by Charbel et al. (1999). Their analysis and conclusions show that, for  $A < 0.014$ , the bed failure mechanism is passive at the spout-annulus interface and the spout is formed slowly from an internal cavity, within which particles circulate. Due to this internal circulation, the cavity is continuously deformed until reaching the bed surface. The free surface of the bed remains horizontal and the spout is maintained stable and centralized in the axial column axis. For  $A > 0.02$ , the bed failure mechanism is active and the spout is formed abruptly in a circular cavity within which few particles oscillate. The free surface of the bed deforms to attain a parabolic shape and the spout

attains stability in the axial column axis at an airflow rate higher than  $1.2 Q_{mj}$ . For  $0.014 \leq A \leq 0.02$ , there is a transitional behavior, meaning that both bed failure mechanisms can occur together and the spout reaches the bed surface abruptly and intermittently. As formed, the spout continues to oscillate around the axial column axis, even at high airflow rates.

Even neglecting the effect of interparticle forces, this simulator predicts well the water evaporating capacity data reported in the literature for spouted bed dryers. Also, as shown by Costa Jr. et al. (2001), the simulated results for drying diluted blood

suspension in conical spouted beds of inert particles are in good agreement with experimental data obtained from the literature. However, it cannot describe the operation of drying concentrated or non-Newtonian suspensions, such as milk emulsion or black liquor. As pointed out by Spitzner Neto and Freire (1997) and corroborated by Medeiros et al. (2001), when non-Newtonian suspensions are used, cohesive forces between inert particles have an expressive influence on airflow, affecting spout formation and stability. Therefore, the simulator developed by Costa Jr. et al. (2001) urges to be reformulated for more general applications.

**Table 1: Gas flow characteristics as a function of bed failure mechanisms, expressed by the range of parameter  $A$  (Costa Jr. et al., 2001).**

Range of $A$	Spout termination mechanism	Spout shape	Gas distribution in the annulus
$A > 0.02$	Fluidization of the top of the bed		
$0.014 \leq A \leq 0.02$	Transitional		
$A < 0.014$	Degeneration of spout into slugs at the base of the bed		

### Effect of Cohesive Forces in Spouted Beds

Passos and Mujumdar (2000) demonstrated that the effect of interaction forces between particles coated by liquid or suspension can be quantified by  $(Q_{mj}/Q_{mj0})$  and  $(\Delta P_{mj}/\Delta P_{mj0})$  ratios. Varying the type and the amount of suspension injected into the bed, the minimum spouting gas-flow rate ( $Q_{mj}$ ) can increase or decrease, greatly or slightly, in relation to that obtained in the bed of dry particles ( $Q_{mj0}$ ). This induces a reduction or an increase in the minimum spouting pressure drop ( $\Delta P_{mj}$ ), compared to that evaluated in the bed of dry particles ( $\Delta P_{mj0}$ ). Therefore, the type of these interaction forces must be directly related to the physical and chemical

suspension properties. In addition, the development and intensity of these forces should depend on the thickness of the suspension layer that covers the particle surface as well as the bed failure mechanism during spout formation.

By using glycerol as a standard coat liquid and working with different inert particles in different spouted bed columns at variety of bed heights, Passos and Mujumdar found expressions for  $(Q_{mj}/Q_{mj0})$  and  $(\Delta P_{mj}/\Delta P_{mj0})$ . As shown in Figure 3,  $(Q_{mj}/Q_{mj0})$  can be well expressed as a function of  $p_1 = e(1-\epsilon_{ag})/\epsilon_{ag}$  and  $(\Delta P_{mj}/\Delta P_{mj0})$  as a function of  $p_2 = e(\phi/d_p)(1-\epsilon_{ag})/\epsilon_{ag}$ . The  $p_1$  and  $p_2$  parameters are those characteristic of the inert particle bed suspension and do not depend on column geometry. Moreover, all

beds of dry inert particles have the same spout formation mechanism, which is expressed by  $A < 0.014$  in conical column geometry. Since the type of interparticle forces depends on the properties of the suspension layer that covers the particles, it is expected that  $(Q_{mj}/Q_{mj0})$  vs.  $p_1$  and  $(\Delta P_{mj}/\Delta P_{mj0})$  vs.  $p_2$  curves differ from one suspension to another. In addition, since the intensity of these forces depends on the contact points between particles and thus the spout formation mechanism, it is expected that these two curves behave differently from one range of parameter  $A$  to another, even for the same suspension. Experiments are in development to confirm these expectations.

Specifically for *Eucalyptus* black liquor, experimental data on  $(Q_{mj}/Q_{mj0})$  and  $(\Delta P_{mj}/\Delta P_{mj0})$ , obtained in conical spouted beds of polypropylene particles with  $A > 0.02$ , confirm that these ratios are functions of  $p_1$  and  $p_2$  within a maximum standard deviation of 10% (see Figure 5).

Because of the complexity of modeling these forces in spouted beds, this work is aimed at developing a methodology to incorporate the effect of interparticle forces into the simulator developed by Costa Jr. et al. (2001) by introducing correction factors into the gas-flow model equations.

### Proposed Methodology

As reported in the literature, the minimum

spouting pressure drop,  $\Delta P_{mj}$ , is associated with gas flowing from the spout to the annulus regions. Therefore, any increase or decrease in  $\Delta P_{mj}$  is due to the increase or reduction in the gas-flow rate through the spout-annulus interface. Therefore,  $\Delta P_{mj}$  and the annular gas-flow rate are directly related. Based on the experimental results obtained in beds of dry particles, any increase in the inlet airflow rate produces an enlargement in spout diameter along the bed height. Therefore, any variation in spout diameter due to the injection of suspension, as shown in Figure 4, must reflect a change in the inlet airflow rate (and conversely).

Evaluating the results in Figure 5, it can be concluded that in beds of polypropylene particles *Eucalyptus* black liquor tends to increase  $Q_{mj}$  to maintain the spouting flow regime. As the amount of liquor rises,  $\Delta P_{mj}$  decreases slightly, reflecting a small reduction in the annulus aeration. Similar trends are also observed in Figure 3; however the increase in  $Q_{mj}$  and the decrease in  $\Delta P_{mj}$  are greater for small ranges of  $p_1$  and  $p_2$ . This behavior is characteristic of the data analyzed here and cannot be extrapolated for another suspension or another range of parameter  $A$ . Medeiros et al. (2001) analyzed in detail the effect of chemical composition of the suspension on the spouting flow regime. Unpublished data on glycerol show that a change in the range of parameter  $A$  (from  $A < 0.014$  to  $0.014 \leq A \leq 0.02$ ) alters the trends observed in Figure 3.

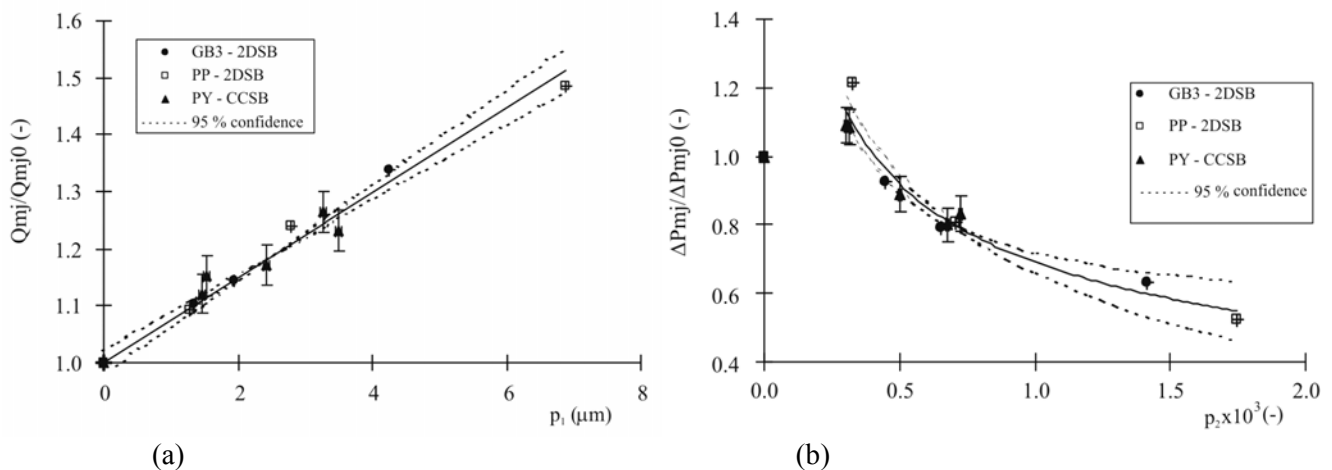


**Figure 3:** Best equations for predicting: (a) the minimum spouting air flow rate ratio as a function of  $p_1 = e(1-\varepsilon_{ag})/\varepsilon_{ag}$  and (b) the minimum spouting pressure drop ratio as a function of  $p_2 = e(\varphi/d_p)(1-\varepsilon_{ag})/\varepsilon_{ag}$  in beds of inert particles coated by glycerol.

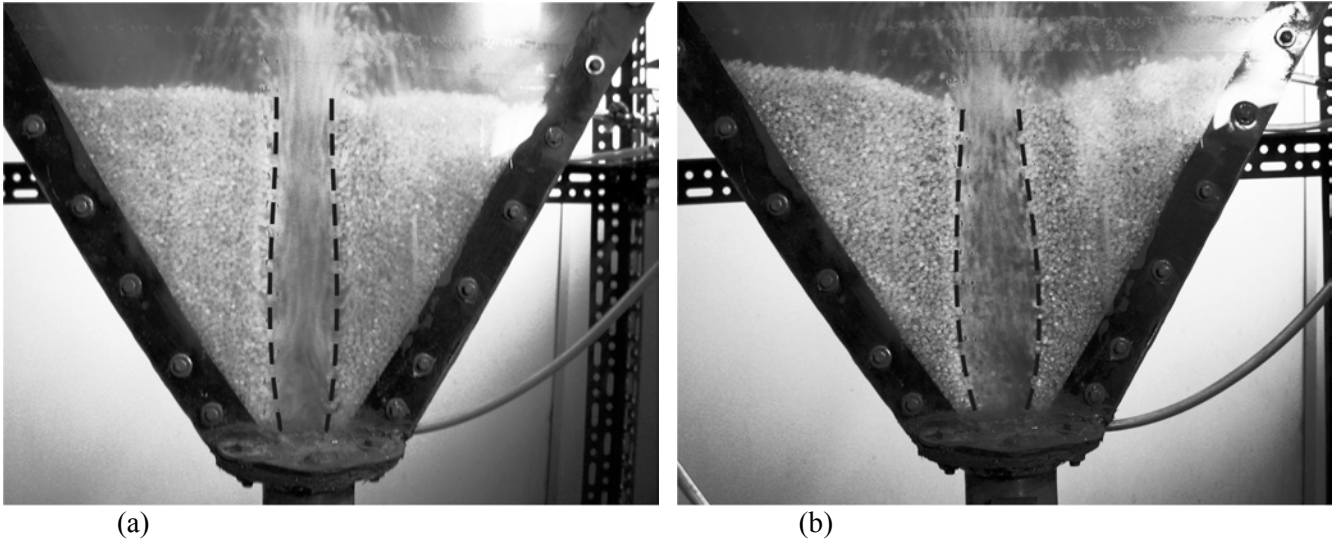


**Figure 4:** Variation in the spout diameter shape as glycerol is added to the bed of inert polypropylene particles in a half-conical spouted bed of  $A = 0.018$ : (a) without glycerol and (b) with 4 ml of glycerol.

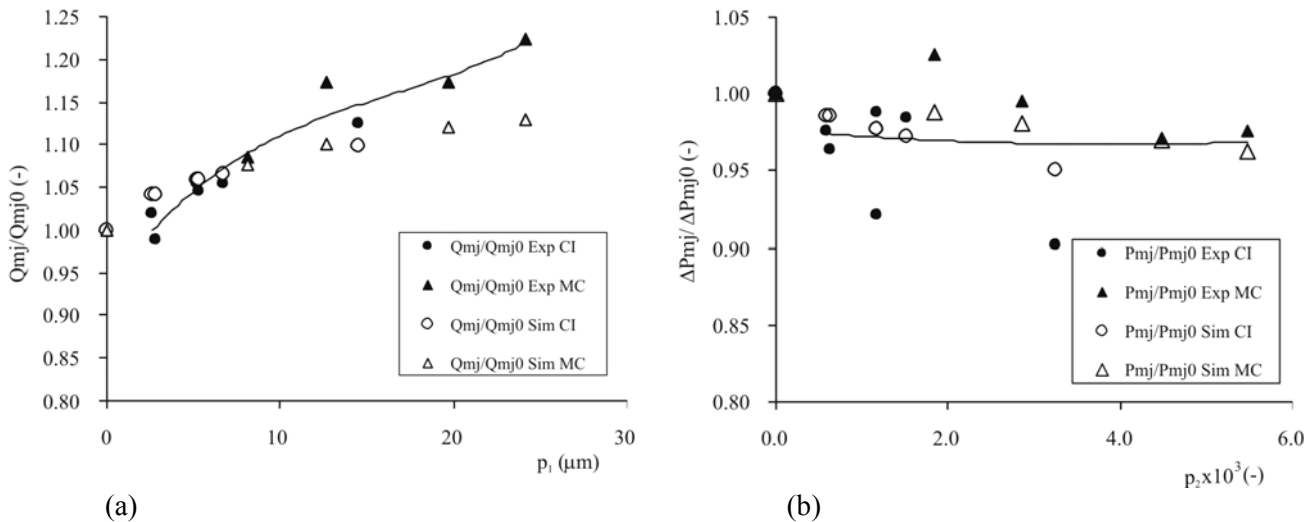


**Figure 5:** Comparison between simulated and experimental data on (a)  $Q_{mj}/Q_{mj0}$  vs.  $p_1$  curve and (b)  $\Delta P_{mj}/\Delta P_{mj0}$  vs.  $p_2$  curve for *Eucalyptus* black liquor.

Focusing on these results, two corrective functions with adjustable parameters are proposed in order to modify the simulator. The first one, called  $f_1$ , is applied to the spout-diameter model equation. This  $f_1$  depends on  $p_1$  and  $z/H$ . The second one, called  $f_2$ , is applied to the rate of airflow that crosses the spout-annulus interface. This  $f_2$  is dependent on  $p_2$  and  $z/H$ . These two functions must attain the unit value in beds without suspension. It is assumed that these functions have the same functional form, since  $f_1$  depends on  $p_1$  and  $f_2$  on  $p_2$ .

The procedure used to determinate the  $f_1$  and  $f_2$  adjustable parameters is the one used in the optimization problem, with the objective function defined as

$$f_{obj} = \sum \left[ (DR_Q)^2 + (DR_P)^2 \right] \quad (2)$$

with

$$DR_Q = \frac{\left[ (Q_{mj}/Q_{mj0})_{sim} - (Q_{mj}/Q_{mj0})_{exp} \right]}{(Q_{mj}/Q_{mj0})_{exp}};$$

$$DR_P = \frac{\left[ (\Delta P_{mj}/\Delta P_{mj0})_{sim} - (\Delta P_{mj}/\Delta P_{mj0})_{exp} \right]}{(\Delta P_{mj}/\Delta P_{mj0})_{exp}}$$

Due to the complexity and the nonlinearity of the gas-flow model equation, the heuristic particle swarm optimization (PSO) method, developed by Kennedy and Eberhart (1995), is chosen to guarantee that the adjustable parameter values obtained are those representative of the global minimum of the objective function. Note that heuristic methods are generally robust and efficient enough to determine the global minimum of the objective function. Parameter restrictions are easily handled in these methods when compared to deterministic methods.

To apply the numerical algorithm to this optimization problem, it is necessary to define the functional form of  $f_1$  and  $f_2$ . This definition is, without any doubt, the most complex step of this methodology and requires additional information about spouted bed behavior with and without suspension, as shown in the next item.

## RESULTS AND DISCUSSION

In Table 2 the experimental values of  $Q_{mj}/Q_{mj0}$  and  $\Delta P_{mj}/\Delta P_{mj0}$  for beds of polypropylene particles covered by *Eucalyptus* black liquor are presented. Some of these data were obtained by Trindade et al. (2000) in a semipilot unit of a conical spouted bed (CI). In a laboratory unit of a half-conical column (MC) Almeida et al. (1999) obtained the rest of these data. In both units, the liquor is injected slowly at the fountain under stable spouting flow regime in beds of dry polypropylene particles. This produces a homogeneous distribution of liquor on particle surfaces. The characteristics and dimensions of these two columns as well as the particle properties are shown in Table 3.

**Table 2: .Experimental data on the minimum spouting conditions in conical spouted beds of polypropylene particles coated by *Eucalyptus* black liquor.**

Exp.	V (ml)	p <sub>1</sub> ( $\mu$ m)	p <sub>2</sub> (-)	$Q_{mj}/Q_{mj0}$ (-)	$\Delta P_{mj}/\Delta P_{mj0}$ (-)
CI1	0	0.00	0.00	1.00	1.00
CI2	5	2.60	0.58	1.02	0.98
CI3	7	5.19	1.16	1.05	0.99
CI4	8	2.80	0.63	0.99	0.96
CI5	10	6.75	1.51	1.05	0.98
CI6	16	5.25	1.18	1.04	0.92
CI7	32	14.50	3.25	1.12	0.90
MC1	0	0.00	0.00	1.00	1.00
MC2	2	8.12	1.80	1.09	1.03
MC3	4	12.62	2.79	1.17	0.99
MC4	6	19.76	4.37	1.17	0.97
MC5	8	24.17	5.35	1.22	0.98

**Table 3: Dimensions of the column and properties of the polypropylene particles used in the experiments.**

Parameter	CI (full column)	MC (half column)
$D_c$ (m)	0.300	0.150
$d_b = d_i$ (m)	0.026	0.013
$\alpha$ ( $^\circ$ )	60	60
M (kg)	2	0.25
H (m)	0.197	0.118
$d_p$ (mm)	0.402	0.412
$\phi$ (-)	0.902	0.912
$\rho_s$ (kg/m <sup>3</sup> )	867	867

As mentioned previously,  $A$  is greater than 0.02 for both units. This means that, in beds of dry particles, bed failure is active and abrupt, annulus aeration is significant at the base of the column and spout diameter expands at the base and remains almost constant in regions near the top of the bed.

Additional information from data reported by Almeida et al. (1999) indicates that the spout diameter near the top of the bed remains quite constant with the injection of low liquor volumes. At  $V = 8$  ml, the spout diameter enlarges. For  $V > 8$  ml, the spout regime is only reached after rigorous agitation of the bed with a glass mixer. In the half-conical column unit, a laboratory compressor supplies air and the inlet air temperature is always lower than the ambient one.

Although in the semipilot unit the spout diameter cannot be visualized, Trindade et al. (2000) observed that the spouting flow regime stops abruptly for  $V > 32$  ml. Under these conditions, a compact inert agglomeration is formed inside the bed (in regions below the free surface of the bed). However, for  $32 \text{ ml} < V \leq 64 \text{ ml}$ , the stable spouting regime is reactivated after 10 minutes of operation, when the powder is removed from the column to the cyclone by exit air. In this semipilot unit, two blowers arranged in series supply air. The inlet air temperature is always higher than ambient temperature. If test operation extends for more than 10 minutes, the inlet air temperature increases up to 40-50°C resulting in the drying of the liquor.

Keeping in mind all this information, the following procedure is used to determine the best form and the best adjustable parameters for  $f_1$  and  $f_2$  functions:

### Step 1

Test different and varied forms of  $f_i(p_i)$ ,  $i = 1$  to 2 and select those that generate the lowest value of the objective function; run the simulator with these functions and compare simulated data on airflow at minimum spouting to the experimental trends. If these trends are satisfied, use these  $f_i$  to modify the airflow model equations in the simulator. If not, go to step 2.

### Step 2

Introduce into  $f_i(p_i)$  the dependence on  $z/H$ , in such a way so as to improve the results obtained in step 1. Test different forms of  $f_i(p_i, z/H)$ ,  $i = 1$  to 2 and select the best functions (lowest value of the objective function); run the simulator with these functions and compare simulated data on airflow at minimum spouting to the experimental trends. If these trends are satisfied, use these  $f_i$  to modify the airflow model equations in the simulator. If not, go to step 3.

### Step 3

Restrain the search space used by the PSO computer algorithm, limiting the range of the adjustable parameters of  $f_i(p_i, z/H)$  functions in step 2. Test different ranges of these parameters; run the simulator with these functions and compare simulated data on airflow at minimum spouting to the experimental trends. Select the functions that best describe the experimental trends and continue to have the lowest value of the objective function.

Results obtained from step 1 are presented in Table 4. For *Eucalyptus* black liquor,  $f_i = 1 + a_i p_i^{c_i}$  ( $i = 1$  to 2) is the best form of all tested to express the dependence of  $f_i$  on  $p_i$ . However, as one can see by  $E_{\text{Max}|p}$ , simulated data on  $(\Delta P_{mj}/\Delta P_{mj0})$  need to be improved. Data on  $U_a/U_{a0}$  along  $z$ , generated by using these  $f_i(p_i)$  functions, shows an increase in annulus aeration as the volume of liquor added to the bed is increased. Also, this  $U_a/U_{a0}$  ratio becomes higher than 1 for regions above the base of the column, resulting in an increase in the simulated value of  $(\Delta P_{mj}/\Delta P_{mj0})$ . Since these results are not in agreement with the experimental trends, step 2 is performed.

Results from step 2 are also presented in Table 4. The best functional form obtained is  $f_i = 1 + \left( a_i \left[ \frac{z}{H} \right] + b_i \right) p_i^{c_i}$  ( $i = 1$  to 2). The objective function as well as all relative errors is minimized. However, as shown in this table, the spout diameter enlarges considerably at the top of the bed as the volume of liquor added to the bed is increased. This is in contrast to trends observed during the experiments. For this reason, step 3 is carried out.

Results from step 3 are also presented in Table 4. The form of  $f_i$  is the same as that obtained in step 2; however its adjustable parameters differ in value. Table 5 displays the new values of these parameters. In Table 4, one can see that this refinement of  $f_i$  functions improves the simulated data on spout diameter in a way that better describes the experimental trends. Note that the simulated spout diameter at the top of the bed contracts slightly as the volume of liquor added to the bed increases, in better agreement with experimental information obtained by Almeida et al. (1999). As the volume of liquor added to the bed is increased, simulated data on  $U_a/U_{a0}$  along  $z$  suggest a reduction in annulus aeration in regions below the bed surface. For  $V = 32$  ml,  $U_a/U_{a0}$  is less than 0.9 at the base of the column, suggesting that particle should first agglomerate near this region. This is in agreement with the experimental observation of Trindade et al. (2000).



**Table 4: Simulated data on airflow at minimum spouting following the procedure used to determine the best  $f_1$  and  $f_2$  functions.**

Corrective function	$r_{mj}(z/H)$	$U_a/U_{a0}(z/H)$
<b>Step 1:</b> $f_i = 1 + a_i p_i^{c_i}$ $i = 1 \text{ to } 2$ $f_{obj} = 0.080$ $E_{M Q} = 5 \%$ $E_{MAX Q} = 10 \%$ $E_{M P} = 5 \%$ $E_{MAX P} = 15 \%$		
<b>Step 2:</b> $f_i = 1 + \left( a_i \left( \frac{z}{H} \right) + b_i \right) p_i^{c_i}$ $i = 1 \text{ to } 2$ $f_{obj} = 0.011$ $E_{M Q} = 1,5 \%$ $E_{MAX Q} = 4 \%$ $E_{M P} = 2 \%$ $E_{MAX P} = 5 \%$		
<b>Step 3:</b> $f_i = 1 + \left( a_i \left( \frac{z}{H} \right) + b_i \right) p_i^{c_i}$ $i = 1 \text{ to } 2$ $f_{obj} = 0.026$ $E_{M Q} = 3 \%$ $E_{MAX Q} = 8 \%$ $E_{M P} = 2 \%$ $E_{MAX P} = 6 \%$		

**Table 5: Adjustable parameters of  $f_1$  and  $f_2$  functions, obtained by step 3.<sup>(\*)</sup>**

<sup>(\*)</sup> Range:  $0.9 < Q_{mj}/Q_{mj0} < 1.3$ ;  $0.9 < \Delta P_{mj}/\Delta P_{mj0} < 1.1$ ;  $0 < e (\mu\text{m}) < 19$ ;  
 No. experimental points = 10; degree of freedom = 4;  
 Exp. standard deviation, maximum value = 10 %.

Function Parameters	$f_i = 1 + \left( a_i \left( \frac{z}{H} \right) + b_i \right) p_i^{c_i}$ $i = 1 \text{ and } 2$
$a_1 (\mu\text{m}^{0.18})$	$-9.18 \times 10^{-1}$
$a_2 (\mu\text{m}/\text{mm}^{-0.507})$	$-9.98 \times 10^{-1}$
$b_1 (\mu\text{m}^{0.18})$	$1.29 \times 10^{-1}$
$b_2 (\mu\text{m}/\text{mm}^{-0.507})$	$3.90 \times 10^{-1}$
$c_1 (-)$	$-1.80 \times 10^{-1}$
$c_2 (-)$	$5.07 \times 10^{-1}$

In Figure 5, simulated and experimental data on  $(Q_{mj}/Q_{mj0})$  and  $(\Delta P_{mj}/\Delta P_{mj0})$  are compared. Simulated errors are lower than experimental errors and within the confidence interval of 95 %.

From this analysis, it can be concluded that the  $f_1$  and  $f_2$  functions obtained in step 3 are adequate to describe the effect of interparticle forces on airflow in conical spouted beds of polypropylene particles coated by *Eucalyptus* black liquor in the range of  $A > 0.02$ .

Figure 6 confirms the reduction in annulus aeration with the increase in volume of liquor added to the bed in regions near the base of the column. As shown, there is a slight increase in this aeration in regions close to the free bed surface ( $z/H > 0.7$ ). Although this increase does not significantly affect the overall value of the  $\Delta P_{mj}/\Delta P_{mj0}$  ratio, it contributes to the liquor drying operation when liquor is injected at the top of the column (as in the cases analyzed here). For this dryer configuration, the liquor layer, which covers the particle surface, is thicker at the top of the bed. This increases the probability of particle agglomeration at the bed surface; however, if agglomerates are formed, they tend to be broken due to the higher annular air velocity in this region. Conversely, in the regions

near the column base, the liquor layer, which covers the particle surface, becomes dry and thinner. This reduces the probability of particle agglomeration in this region. However, when the inlet liquor flow rate is increased up to a specific value, the thinning of the liquor layer due to the drying operation is not enough to avoid particle agglomeration. Under this condition, the spouting regime ceases because agglomerates formed near the base of the column are preserved (annulus aeration is lower in this region to promote agglomerate breakage). This behavior, suggested by simulated data on  $U_a(z/H)$ , may explain the abrupt collapse of the spouting regime in the semipilot unit at  $V > 32$  ml and the reactivation of the spouting regime 10 minutes after injection of the liquor.

Figure 7 contains simulated data on the pressure drop profile along  $z$  at the spout-annulus interface. This corroborates the experimental data information that changes in this profile with the liquor are insignificant at  $z = H$  (top of the bed). Moreover, for high values of  $V$ , the pressure drop at the spout-annulus interface decreases at  $z/H \leq 0.4$ , confirming the slight decrease in  $\Delta P_{mj}$  with the increase in  $V$ . Note that  $\Delta P_{mj}$  is the integrated value of  $\Delta P_j$  along the bed height.

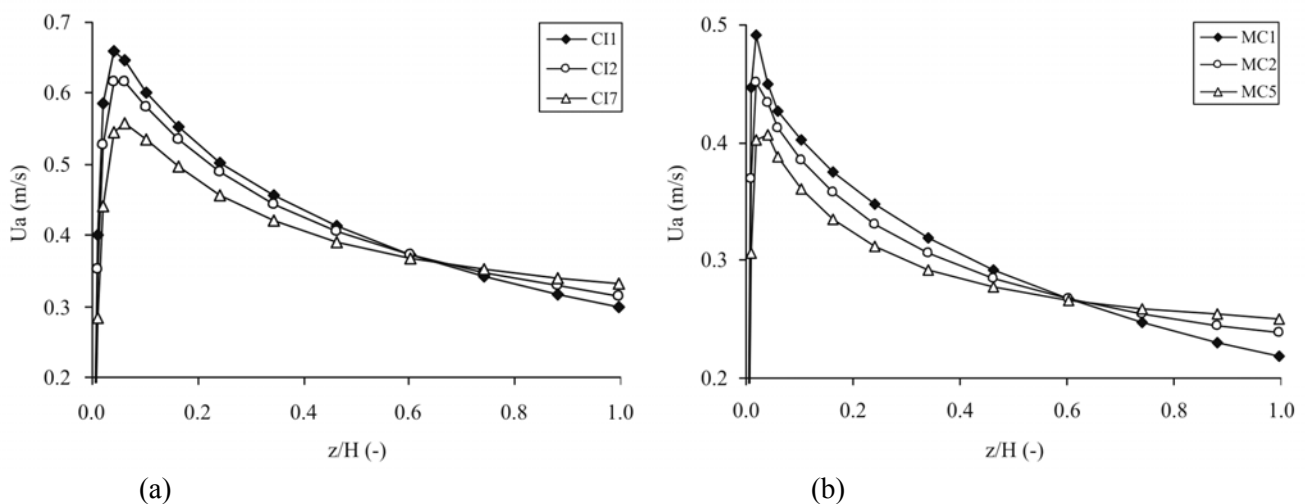


**Figure 6:** Simulated data on superficial air velocity in the annulus region along the bed height for experimental conditions given in Table 2: (a) half-conical spouted bed and (b) full conical spouted bed.

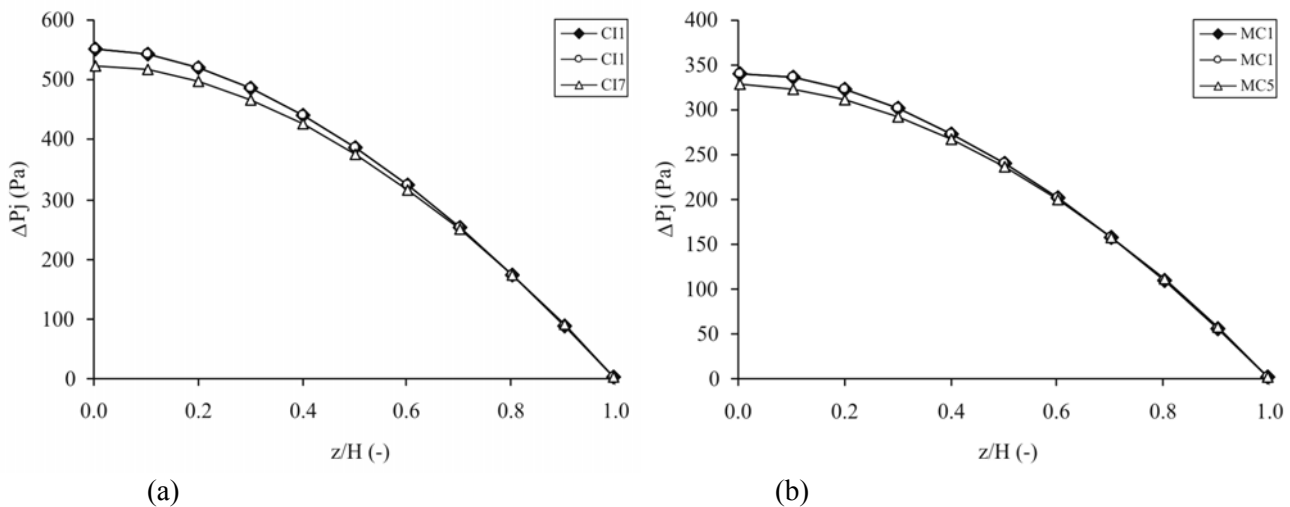


**Figure 7:** Simulated data on pressure drop along the spout-annulus interface for experimental conditions given in Table 2: (a) half-conical spouted bed and (b) full conical spouted bed.

## CONCLUSIONS

Based on the results and discussion presented, the methodology proposed in this work to introduce the effect of interparticle forces into the simulator developed by Costa Jr. et al. (2001) is coherent, efficient and promising. Results obtained for the airflow distribution and spout diameter in conical spouted beds of polypropylene particles coated by *Eucalyptus* black liquor are in agreement with experimental data and observations. This demonstrates that the corrective functions proposed adequately incorporate the effect of cohesive forces between these particles within the experimental variable range analyzed. These corrective functions, introduced into the simulator, improve considerably the data simulation for *Eucalyptus* black liquor. This modified simulator is used to predict the liquor drying operation in the semipilot unit.

In parallel, work is being developed to apply this methodology to other suspensions and spouted bed columns. This will contribute to a generalization of results presented here.

## ACKNOWLEDGEMENTS

Authors are grateful to the Conselho Nacional de Desenvolvimento Científico e Tecnológico (CNPq) and the Fundação de Amparo à Pesquisa do Estado de Minas Gerais (FAPEMIG) for their financial support and to CENIBRA for providing the liquor samples used.

## NOMENCLATURE

$a_1$	adjustable parameter of $f_1$	$m^{c1}$
$a_2$	adjustable parameter of $f_2$	-
A	parameter defined in Equation (1)	-
$b_1$	adjustable parameter of $f_1$	$m^{c1}$
$b_2$	adjustable parameter of $f_2$	-
$c_1$	adjustable parameter of $f_1$	-
$c_2$	adjustable parameter of $f_2$	-
$C_{ss}$	liquor solids concentration (mass of dry solids per mass of suspension)	-
$d_b$	diameter of the column base	m
$d_i$	inlet nozzle diameter	m
$d_j$	spout diameter	m
$d_{mj}$	spout diameter just above the minimum spouting condition	m
$d_p$	particle diameter	mm; m
$D_c$	column diameter	m
$DR_1$	relative deviation of $Q_{mj} = [(Q_{mj}/Q_{mj0})_{sim} - (Q_{mj}/Q_{mj0})_{exp}] / (Q_{mj}/Q_{mj0})_{exp}$	-
$DR_1$	relative deviation of $\Delta P_{mj} = [(\Delta P_{mj}/\Delta P_{mj0})_{sim} - (\Delta P_{mj}/\Delta P_{mj0})_{exp}] / (\Delta P_{mj}/\Delta P_{mj0})_{exp}$	-
e	thickness of liquid layer covering one particle	$\mu m$
$E_M$	mean relative error	-
$E_{MAX}$	maximum relative error	-
$f_1$	corrective function for the spout diameter	-

$f_2$	corrective function for the superficial velocity of gas flowing through the annulus-spout interface	-	$\varepsilon_{ag}$	actual void space for fluid flowing through the wet bed in the annulus	-
$f_{obj}$	objective function for optimization	-	$\varepsilon_{mf}$	bed porosity under the minimum fluidization condition	-
$g$	gravity acceleration	$m/s^2$	$\varphi$	particle sphericity	-
$H$	bed height	$m$	$\eta$	apparent viscosity of the liquor	$mPa \cdot s$
$H_L$	height of the lateral column area through which air is introduced into bed	$m$	$\rho_f$	gas density	$kg/m^3$
$n$	number of segments in which the bed of particles is divided	-	$\rho_s$	solid density (inert particles)	$kg/m^3$
$M$	mass of inert particles inside the column	$kg$	<b>Symbols</b>		
$p_1$	$= e (1-\varepsilon_{ag})/\varepsilon_{ag}$	$\mu m$	2DSB	two-dimensional spouted bed	
$p_2$	$= e (\varphi/d_p) (1-\varepsilon_{ag})/\varepsilon_{ag}$	-	CCBS	conical spouted bed	
$P$	pressure	$Pa$	CI full	conical column	
$Q_{mj}$	gas flow rate at minimum spouting	$m^3/s$	GB3	glass beads	
$Q_{mj0}$	gas flow rate at minimum spouting for beds of dry particles	$m^3/s$	MC	half-conical column	
$r_{mj}$	spout radius at minimum spouting ( $= d_{mj}/2$ )	$m$	PP	plastic pellets	
$T$	temperature	$^{\circ}C$	PY	polypropylene particles	
$U_a$	gas superficial velocity in the annulus region	$m/s$	<b>REFERENCES</b>		
$U_{a0}$	gas superficial velocity in the annulus region for beds of dry particles	$m/s$	Almeida, A.P.P., Cançado, F.L., Duarte, I.S., Baumgartl, L.O., Vitorino, M.D., Gomes, R.C., Abreu, W.M., Passos, M.L. and d'Angelo, J.V.H., Study of Fluid Flow in a Conical Spouted Bed for Drying the Eucalyptus Black Liquor, 3 <sup>o</sup> Congresso Brasileiro de Engenharia Química em Iniciação Científica, Belo Horizonte, CD-ROM (1999).		
$U_{ao(i)}$	gas superficial velocity at the entrance of the i segment of the bed	$m/s$	Cardoso, M., Analysis of the Eucalyptus Black Liquor Recovery in the Kraft Process for Evaluating Alternative Processing Routes, Ph.D. diss., UNICAMP, Campinas (1998).		
$U_{aH(i)}$	gas superficial velocity at the exit of the i segment of the bed	$m/s$	Charbel, A.L.T.; Massarani, G. and Passos, M.L., Analysis of Effective Solid Stresses in a Conical Spouted Bed, Brazilian J. of Chemical Engineering, 16, p. 433 (1999).		
$U_j$	gas superficial velocity in the spout region	$m/s$	Costa Jr., E.F., Cardoso, M. and Passos, M.L., Simulation of Drying Suspension in Spout-Fluid Beds of Inert Particles, Drying Tech. J., 19, p. 1975 (2001).		
$U_{mf}$	gas superficial velocity at minimum fluidization	$m/s$	Green, R.P. and Hough, G. (Eds.), Chemical Recovery in the Alkaline Pulping Processes, TAPPI Press, Salem (1992).		
$U_T$	terminal particle velocity	$m/s$	Hyoty, P.A. and Ojala, S.T., High-solids Black Liquor Combustion, TAPPI Journal, 71, No. 1, p.108 (1988).		
$V$	volume of suspension added to the bed of particles	$ml$	Kennedy, J. and Eberhart, R.C., Particle Swarm Optimization, International Conference on Neural Networks. Perth, Australia (1995).		
$z$	axial coordinate of the column	$m$			

**Greek Symbols**

$\alpha$	included column angle	
$\Delta P_j$	spout-annulus interface pressure drop = $P_j(z) - P_j(z = H)$	$Pa$
$\Delta P_{mj}$	minimum spouting pressure drop	$Pa$
$\Delta P_{mjo}$	minimum spouting pressure drop in beds of dry particles	$Pa$
$\varepsilon$	bed porosity	-
$\varepsilon_a$	bed porosity in the annulus region	-

- Littman, H. and Morgan, M.H., Transport Processes in Fluidized Beds, Elsevier, Amsterdam, p. 287 (1988).
- Medeiros, M.F.D., Alsina, O.L.S., Rocha, S.C., Jerônimo, C.E.M., Mata, A.L.M., Medeiros, U.K.L. and Furtunato, A.A., Flowing of Beds of Inert Particles with Tropical Fruit Pulp: Effects on Drying Operation in Spouted Beds, Rev. Bras. de Engenharia Agrícola e Ambiental, 5, p. 475 (2001).
- Passos, M.L. and Mujumdar, A.S., Effect of Cohesive Forces on Fluidized and Spouted Beds of Wet Particles, Powder Techn., 110, p. 222 (2000).
- Passos, M.L., d'Angelo, J.V.H. and Mujumdar, A.S., Effect of Capillary Forces on the Drying of Non-Newtonian Suspension in Fluid Beds of Inert Particles, 12<sup>th</sup> International Drying Symposium, CD-ROM, p. 202, Elsevier, Holland (2000).
- Smook, J.A., Handbook for Pulp and Paper Technologies, Angus-Wilde, Vancouver (1992).
- Spitzner Neto, P.I. and Freire, J.T., Studies of Drying Pastes in Spouted Beds: Influence of the Presence of Paste on the Process, XXV Congresso Brasileiro de Sistemas Particulados, UFSCar, São Carlos, 1, p.185 (1997).
- Trindade, A.L.G., d'Angelo, J.V.H. and Passos, M.L., Characterization of Powder Product from the Black Liquor Drying in Spouted Beds and Process Optimization, 14<sup>o</sup> Congresso Brasileiro de Engenharia Química, UFRN, Natal, CD-ROM (2002).
- Trindade, A.L.G., Passos, M.L. and d'Angelo, J.V.H., Drying Simulation of *Eucalyptus* Black Liquor in Spout-Fluid Beds, IX Semana de Iniciação Científica, p.391, UFMG, Belo Horizonte (2000).